

Two electrons in harmonic confinement coupled to light in a cavity

Chenhang Huang,¹ Alexander Ahrens,¹ Matthew Beutel,¹ and Kálmán Varga^{1,*}

¹*Department of Physics and Astronomy, Vanderbilt University, Nashville, Tennessee, 37235, USA*

The energy and wave function of a harmonically confined two-electron system coupled to light is calculated by separating the wave functions of the relative and center of mass (CM) motions. The relative motion wave function has a known quasi-analytical solution. The light only couples to the CM variable and the coupled equation can be solved with diagonalization without approximations. The approach works for any coupling strength. Examples of wave functions of light-matter hybrid states are presented.

I. INTRODUCTION

Analytically or numerically easily solvable systems (e.g. by "exact diagonalization") have always been important test grounds for models and approximations. Recently, there is an intense interest in strongly coupled light-matter systems^{1–15}. In these systems, the light-matter coupling cannot be treated perturbatively. The electronic excitations and the photons are superimposed, forming hybrid light-matter excitations. In this regime, there are only a few analytical approaches available to test and develop efficient numerical methods. Reviews of the recent theoretical and experimental development can be found in Refs.^{16–18}.

In this paper, we consider a two-electron system interacting via the Coulomb interaction, confined by a harmonic oscillator interaction coupled to light in a cavity. The system is described on the level of the Pauli-Fierz (PF) nonrelativistic QED Hamiltonian. The two-electron system in harmonic oscillator confinement is a quasi-exactly solvable (QES) problem. The wave function can be written as a product of the wave functions of the relative and CM motion. The relative motion wave function can be expanded into infinite series. For certain oscillator parameters, this infinite series can be reduced to a recursion¹⁹. The wave function of the CM motion is a simple harmonic oscillator eigenfunction. We will show that the photons only couple to the CM coordinate and the coupled CM photon system can be solved by exact diagonalization.

The two-particle systems have long been investigated due to their analytic and quasi-exact solvability, which provides straightforward intuition for the physical system under scrutiny as well as an excellent benchmark test for numerical computations. Examples of QES quantum systems are the two-dimensional (2D) harmoniums^{19,20} and the hydrogen-like atoms in homogeneous magnetic fields²¹. These QES problems have been generalized to relativistic cases as well^{22,23}. For harmonium systems, the separability condition guarantees the quasi-exact solvability for the Schrödinger equation²⁴, and linearly coupled oscillators have been studied under this condition²⁵. For hydrogen-like models, solutions have been found for particular forms of the inhomogeneous magnetic fields^{26,27}. Examples of other known QES models include the planar Dirac electron in hydrogen-

like atoms^{28,29}, one-body problems in power-law central potentials^{30,31}, relativistic 2D pion in constant magnetic fields³², and 1D and 3D regularized Calogero models^{33,34}. QES models with different forms of confinements, e.g. two electrons in one³⁵ or two³⁶ 1D rings, two electrons on the surface of the n-sphere (spherium)^{37,38}, have also been studied.

The exact or even the numerical solution for light-matter coupled systems is very difficult even on the level of a minimal coupling Hamiltonian in the long-wavelength limit³⁹, because the photons substantially increase the number degrees of freedom of the system. Theoretical approaches have been developed to tame the light-matter coupled systems using approximations and transformations^{15,15,39–43,43,43–48}. In Refs.^{41,42}, an electron in a 2D potential coupled to a single photon mode is used as a numerical benchmark test. The spatial part of the wave function is represented on a real space grid and coupled to the Fock space of the photons. The Hamiltonian of the system can be diagonalized in this representation and the light coupled wave function can be studied. In Ref.⁴³, the spatial wave function of the He, HD⁺, and H₂⁺ three-particle system is represented using a 3D product of pseudospectral basis functions, and a few Fock spaces states of a single photon mode are coupled to the spatial part. The energy and wave function is calculated by exact diagonalization of the PF Hamiltonian and the Jaynes–Cummings limit for electronic and ro-vibrational transitions are studied. One-dimensional model systems of atoms and molecules^{1,44} often using the Shin-Metiu potential⁴⁹ are also useful to describe potential energy surfaces in cavities and test numerical approaches.

The free electron gas also allows analytical treatment⁴⁸. In Ref.⁴⁸, the free electron gas in cavity is analytically solved in the long-wavelength limit for an arbitrary number of non-interacting electrons. It is found that the electron-photon ground state is a Fermi liquid containing virtual photons.

Approaches to reformulating the problem have also been proposed. In Ref.¹⁵, the light and matter degrees of freedom are decoupled using a unitary transformation. In the transformed frame, both the light and the matter Hilbert spaces can be truncated systematically to facilitate an efficient solution. In Ref.⁷ a variational formulation is developed and the semianalytical formula is derived for the ground and excited state energies.

II. FORMALISM

We consider two particles with positions \mathbf{r}_1 , \mathbf{r}_2 and charges q_1 , q_2 . Later we show that an analytical approach only works for $q_1 = q_2$, but it is useful to consider the general case to show the origin of the coupling to the center of mass. The Hamiltonian of the system is

$$H = H_e + H_{ph} = H_e + H_p + H_{ep} + H_d. \quad (2.1)$$

H_e is the electronic Hamiltonian, H_{ph} describes the electron-photon interaction, which is a sum of three terms, the photon Hamiltonian H_p , the electron-photon coupling H_{ep} , and the dipole self-interaction H_d . The electron-photon interaction can be described by using the PF nonrelativistic QED Hamiltonian. The PF Hamiltonian can be rigorously derived^{3,6,10,12,50} by applying the Power-Zienau-Woolley gauge transformation⁵¹, with a unitary phase transformation on the minimal coupling ($p \cdot A$) Hamiltonian in the Coulomb gauge,

$$H_{ph} = \frac{1}{2} \sum_{\alpha=1}^{N_p} \left[p_{\alpha}^2 + \omega_{\alpha}^2 \left(q_{\alpha} - \frac{\boldsymbol{\lambda}_{\alpha}}{\omega_{\alpha}} \cdot \mathbf{D} \right)^2 \right], \quad (2.2)$$

where $\mathbf{D} = \sum_{i=1}^N q_i \mathbf{r}_i$ is the dipole operator. The photon fields are described by quantized oscillators. $q_{\alpha} = \frac{1}{\sqrt{2\omega_{\alpha}}}(\hat{a}_{\alpha}^+ + \hat{a}_{\alpha})$ is the displacement field and $p_{\alpha} = -i\sqrt{\frac{\omega_{\alpha}}{2}}(\hat{a}_{\alpha} - \hat{a}_{\alpha}^+)$ is the conjugate momentum. This Hamiltonian describes N_p photon modes with frequency ω_{α} and coupling $\boldsymbol{\lambda}_{\alpha}$. The coupling term is usually written as⁵²

$$\boldsymbol{\lambda}_{\alpha} = \sqrt{4\pi} S_{\alpha}(\mathbf{r}) \mathbf{e}_{\alpha}, \quad (2.3)$$

where $S_{\alpha}(\mathbf{r})$ is the mode function at position \mathbf{r} and \mathbf{e}_{α} is the transversal polarization vector of the photon modes.

The three components of the electron-photon interaction are as follows: The photonic part is

$$H_p = \sum_{\alpha=1}^{N_p} \left(\frac{1}{2} p_{\alpha}^2 + \frac{\omega_{\alpha}^2}{2} q_{\alpha}^2 \right) = \sum_{\alpha=1}^{N_p} \omega_{\alpha} \left(\hat{a}_{\alpha}^+ \hat{a}_{\alpha} + \frac{1}{2} \right). \quad (2.4)$$

By using the creation and annihilation operators, the photon states $|n_{\alpha}\rangle$ can be generated by multiple applications of the creation operators on the vacuum state $|n_{\alpha}\rangle = (\hat{a}_{\alpha}^+)^n |0\rangle$. All other photon operations can be done by using \hat{a}_{α} and \hat{a}_{α}^+ . The interaction term is

$$H_{ep} = - \sum_{\alpha=1}^{N_p} \omega_{\alpha} q_{\alpha} \boldsymbol{\lambda}_{\alpha} \cdot \mathbf{D} = - \sum_{\alpha=1}^{N_p} \sqrt{\frac{\omega_{\alpha}}{2}} (\hat{a}_{\alpha} + \hat{a}_{\alpha}^+) \boldsymbol{\lambda}_{\alpha} \cdot \mathbf{D}. \quad (2.5)$$

Only photon states $|n_{\alpha}\rangle$, $|n_{\alpha} \pm 1\rangle$ are connected by \hat{a}_{α} and \hat{a}_{α}^+ . The matrix elements of the dipole operator \mathbf{D} are only nonzero between spatial basis functions with angular momentum l and $l \pm 1$ in 3D or m and $m \pm 1$ in 2D. The strength of the electron-photon interaction can be

characterized by the effective coupling parameter

$$g_{\alpha} = |\boldsymbol{\lambda}_{\alpha}| \sqrt{\frac{\omega_{\alpha}}{2}}. \quad (2.6)$$

The dipole self-interaction is

$$H_d = \frac{1}{2} \sum_{\alpha=1}^{N_p} (\boldsymbol{\lambda}_{\alpha} \cdot \mathbf{D})^2, \quad (2.7)$$

which describes the effects of the polarization of the electrons back on the photon field. The importance of this term for the existence of a ground state is discussed in Ref⁶.

A. Separation of the relative and center of mass equations

For simplicity we only consider a single photon mode. The formalism can be easily extended to many photon modes as described in Appendix A and Appendix B. We will define the coupling strength as $\boldsymbol{\lambda} = (\lambda, \lambda, 0)$. A more general case is described in Appendix B. In this section, we consider the Hamiltonian that acts only in the electron space

$$H_e + H_d = -\frac{1}{2} \nabla_1^2 + \frac{1}{2} \omega_0^2 \mathbf{r}_1^2 - \frac{1}{2} \nabla_2^2 + \frac{1}{2} \omega_0^2 \mathbf{r}_2^2 + \frac{q_1 q_2}{|\mathbf{r}_1 - \mathbf{r}_2|} + \frac{1}{2} (q_1 \boldsymbol{\lambda} \cdot \mathbf{r}_1 + q_2 \boldsymbol{\lambda} \cdot \mathbf{r}_2)^2. \quad (2.8)$$

Atomic units $\hbar = m = e = 1$ are used throughout and unit charges are assumed.

Defining relative and CM coordinates as

$$\begin{aligned} \mathbf{r} &= \mathbf{r}_2 - \mathbf{r}_1, \\ \mathbf{R} &= \frac{1}{2} (\mathbf{r}_1 + \mathbf{r}_2), \end{aligned} \quad (2.9)$$

the Hamiltonian decouples into a relative and CM Hamiltonian

$$\begin{aligned} H_e + H_d &= -\nabla_{\mathbf{r}}^2 + \frac{1}{4} \omega_0^2 \mathbf{r}^2 + \frac{q_1 q_2}{r} - \frac{1}{4} \nabla_{\mathbf{R}}^2 + \omega_0^2 \mathbf{R}^2 \\ &+ \frac{1}{2} \left(\boldsymbol{\lambda} \cdot \left((q_1 + q_2) \mathbf{R} + \frac{1}{2} (q_1 - q_2) \mathbf{r} \right) \right)^2 \\ &\equiv H_{\mathbf{r}} + H_{\mathbf{R}}, \end{aligned} \quad (2.10)$$

and the corresponding eigenvalue problem is

$$(H_{\mathbf{r}} + H_{\mathbf{R}}) \Phi(\mathbf{r}, \mathbf{R}) = (\epsilon + \eta) \Phi(\mathbf{r}, \mathbf{R}), \quad (2.11)$$

and $E = \epsilon + \eta$ is the eigenenergy. Note that for like charges, the last term only contributes to $H_{\mathbf{R}}$, otherwise, it only contributes to $H_{\mathbf{r}}$ and there is no cross term between \mathbf{R} and \mathbf{r} .

1. $q_1 = -q_2$

In this case the photon only couples to $\mathbf{r} = (x, y, z)$. The CM wave function is a harmonic oscillator eigenfunction with frequency $2\omega_0$. By introducing $u = \frac{x+y}{\sqrt{2}}$, and $v = \frac{-x+y}{\sqrt{2}}$, the relative motion Hamiltonian takes the form

$$H_{\mathbf{r}} = -\nabla_u^2 - \nabla_v^2 - \nabla_z^2 + \frac{1}{2}\omega_u^2 u^2 + \frac{1}{2}\omega_v^2 v^2 + \frac{1}{2}\omega_z^2 z^2 - \frac{1}{(u^2 + v^2 + z^2)^{1/2}}, \quad (2.12)$$

where $\omega_u^2 = 2\lambda^2 + \frac{1}{2}\omega_0^2$, $\omega_v^2 = \omega_z^2 = \frac{1}{2}\omega_0^2$. This is a single particle Coulomb problem in an anisotropic harmonic potential. The derivation is detailed in the next section. We are not aware of any existing analytical solutions to this system. One can, in principle, solve this problem using a product basis of the $u - v - z$ harmonic oscillators, but we do not pursue this case any further in this paper.

2. $q_1 = q_2$

In the following, we will consider $q_1 = q_2$ because, in this case, the equation for the relative motion can be analytically found for certain frequencies as mentioned before. After multiplying the relative part by $1/2$ and the CM part by 2 to bring the equations in a more convenient form, we have

$$\left[-\frac{1}{2}\nabla_{\mathbf{r}}^2 + \frac{1}{2}\omega_{\mathbf{r}}^2 \mathbf{r}^2 + \frac{1}{2r} \right] \varphi(\mathbf{r}) = \varepsilon' \varphi(\mathbf{r}), \quad (2.13)$$

where $\omega_{\mathbf{r}} = \frac{1}{2}\omega_0$ and $\varepsilon' = \frac{1}{2}\varepsilon$, and

$$\left[-\frac{1}{2}\nabla_{\mathbf{R}}^2 + \frac{1}{2}\omega_{\mathbf{R}}^2 \mathbf{R}^2 + 4(\boldsymbol{\lambda} \cdot \mathbf{R})^2 \right] \xi(\mathbf{R}) = \eta' \xi(\mathbf{R}), \quad (2.14)$$

where $\omega_{\mathbf{R}} = 2\omega_0$ and $\eta' = 2\eta$. The total wave function can be written as

$$\Phi(\mathbf{r}, \mathbf{R}) = \varphi(\mathbf{r})\xi(\mathbf{R}). \quad (2.15)$$

In this case, the CM motion in the z -direction is described by a harmonic oscillator eigenfunction, and we drop this part from now.

In 2D, using $\mathbf{R} = (X, Y)$ one can rewrite $H_{\mathbf{R}}$ as (in 3D one simply has to multiply the CM wave function with a harmonic oscillator function of frequency $2\omega_0$ in the Z direction)

$$H_{\mathbf{R}} = -\frac{1}{2}\frac{\partial^2}{\partial X^2} - \frac{1}{2}\frac{\partial^2}{\partial Y^2} + \frac{1}{2}\omega_X^2 X^2 + \frac{1}{2}\omega_Y^2 Y^2 + \frac{1}{2}\omega_{XY}^2 XY, \quad (2.16)$$

where

$$\omega_X^2 = \omega_Y^2 = \omega_{\mathbf{R}}^2 + 8\lambda^2, \quad \omega_{XY}^2 = 16\lambda^2. \quad (2.17)$$

Using a unitary transformation (a generalized version is presented in Appendix A)

$$U = \frac{X+Y}{\sqrt{2}}, \quad V = \frac{-X+Y}{\sqrt{2}}, \quad (2.18)$$

we have

$$H_{\mathbf{R}} = -\frac{1}{2}\frac{\partial^2}{\partial U^2} - \frac{1}{2}\frac{\partial^2}{\partial V^2} + \frac{1}{2}\omega_U^2 U^2 + \frac{1}{2}\omega_V^2 V^2 \equiv H_U + H_V, \quad (2.19)$$

where

$$\omega_U^2 = \frac{1}{2}(\omega_X^2 + \omega_{XY}^2 + \omega_Y^2) = \omega_{\mathbf{R}}^2 + 16\lambda^2, \quad (2.20)$$

$$\omega_V^2 = \frac{1}{2}(\omega_X^2 - \omega_{XY}^2 + \omega_Y^2) = \omega_{\mathbf{R}}^2. \quad (2.21)$$

This Hamiltonian is analytically solvable: the lowest energy is

$$\eta = \frac{1}{2} \left(\omega_0 + \sqrt{\omega_0^2 + 4\lambda^2} \right). \quad (2.22)$$

$H_{\mathbf{r}}$ is also analytically solvable, in this case, for certain frequencies^{19,53}. For example, for $\omega_0 = 1$ one gets $\varepsilon = 2$ (see the Table in Ref.⁵³) and the total energy is $E = 2 + \frac{1}{2} + \frac{1}{2}\sqrt{1 + 4\lambda^2}$.

The wave function of the CM motion now can be written as

$$\xi(\mathbf{R}) = \phi_k(U)\phi_l(V), \quad (2.23)$$

where ϕ_k is the k th eigenfunction of the one-dimensional harmonic oscillator,

$$\phi_k(U) = \left(\frac{\sqrt{\omega_U}}{\sqrt{\pi} 2^k k!} \right)^{\frac{1}{2}} e^{-\frac{\omega_U}{2} U^2} H_k(\sqrt{\omega_U} U), \quad (2.24)$$

and the eigenfunctions are similarly defined for V .

B. Photon-electron coupling

The coupling term Eq. (2.5) takes the form

$$H_{ep} = -\sqrt{\frac{\omega}{2}}(\hat{a} + \hat{a}^+)\lambda D, \quad D = 2\sqrt{2}U, \quad (2.25)$$

so only the U harmonic oscillators are coupled with photons. The Hamiltonian that we have to solve is reduced to a single one-dimensional electronic Hamiltonian coupled to light:

$$H_c = H_U + \omega \left(\hat{a}^+ \hat{a} + \frac{1}{2} \right) - 2\omega\sqrt{2}\lambda U q. \quad (2.26)$$

This Hamiltonian can be solved by exact diagonalization using the basis states

$$\phi_k(U)|n\rangle. \quad (2.27)$$

For the diagonalization, one needs the matrix elements of the Hamiltonian which are readily available. The operators H_U and U act on the real space, and $\hat{a} + \hat{a}^+$ acts on the photon space. For the coupling term in the photon space:

$$\begin{aligned} q|n\rangle &= \frac{1}{\sqrt{2\omega}} (\hat{a} + \hat{a}^+) |n\rangle \\ &= \frac{1}{\sqrt{2\omega}} (|\sqrt{n}|n-1\rangle + \sqrt{n+1}|n+1\rangle), \end{aligned} \quad (2.28)$$

and the matrix elements of q are

$$\langle m|q|n\rangle = \frac{1}{\sqrt{2\omega}} D_{mn}, \quad (2.29)$$

where

$$D_{mn} = \begin{pmatrix} 0 & \sqrt{1} & 0 & 0 & 0 & \dots \\ \sqrt{1} & 0 & \sqrt{2} & 0 & 0 & \dots \\ 0 & \sqrt{2} & 0 & \sqrt{3} & 0 & \dots \\ 0 & 0 & \sqrt{3} & 0 & \sqrt{4} & \dots \\ 0 & 0 & 0 & \sqrt{4} & 0 & \dots \\ \vdots & \vdots & \vdots & \vdots & \vdots & \ddots \end{pmatrix}. \quad (2.30)$$

$$\langle m, \phi_i|H_c|n, \phi_j\rangle = \delta_{mn}\delta_{ij}(j + \frac{1}{2})\omega_U + \delta_{mn}\delta_{ij}(n + \frac{1}{2})\omega + \sqrt{\frac{2\omega}{\omega_U}} \lambda D_{mn}D_{ij}. \quad (2.34)$$

This is a very sparse matrix and can be diagonalized with sparse matrix approaches even for very large dimensions. In practice, a few dozen photon bases $|n\rangle$ and harmonic oscillator bases ϕ_i give converged energies. This matrix is generalized for N_p photon modes in Appendix A.

After the diagonalization, we have the eigenenergies η'_j and the eigenfunctions by defining the spatial wave function in the photon subspace n as

$$\psi_j(\mathbf{R}) = \phi_0(V)\phi_j(U), \quad (2.35)$$

the eigenfunction for the CM motion is

$$\begin{aligned} \xi_k(\mathbf{R}) &= \sum_{n=0}^{K_n} \left(\sum_{j=0}^{K_U} c_{j,n}^k \psi_n(\mathbf{R}) \right) |n\rangle \\ &= \sum_{j=0}^{K_U} \left(\sum_{n=0}^{K_n} c_{j,n}^k |n\rangle \right) \psi_j(\mathbf{R}), \end{aligned} \quad (2.36)$$

where K_U and K_n are some suitably chosen upper limits that control the convergence of the eigenvalues. For the V part of the CM motion, we have chosen the lowest state. The first line in Eq. (2.36) emphasizes the

The Hamiltonian H_U is diagonal in the harmonic oscillator bases

$$\langle \phi_i|H_U|\phi_j\rangle = (j + \frac{1}{2})\omega_U\delta_{ij}. \quad (2.31)$$

The matrix elements of the photon Hamiltonian are

$$\langle n|\omega \left(\hat{a}^+\hat{a} + \frac{1}{2} \right) |m\rangle = (n + \frac{1}{2})\omega\delta_{nm}. \quad (2.32)$$

The last piece is the matrix elements of the position operator in harmonic oscillator bases:

$$\langle \phi_i|U|\phi_j\rangle = \frac{1}{\sqrt{2\omega_U}} D_{ij}. \quad (2.33)$$

Thus, the matrix elements of H_c are

coupling of the spatial part to photon spaces; the second line emphasizes the coupling of the linear combination of photon states to a given CM eigenfunction.

III. RESULTS AND DISCUSSION

A few examples will be presented in this section. For these calculations, we have picked an oscillator frequency ω_0 from the Table of Ref.⁵³, calculated the radial part of the relative wave function as described in Refs.^{19,20,53}, and multiplied with the corresponding spherical function. This function is then multiplied by $\xi_k(\mathbf{R})$ calculated using Eq. (2.36).

First, we show the wave function for the different CM excitation. In this case, two variables determine the behavior: the confining strength ω_0 and the coupling parameter λ . We show 2D examples because they are easier to visualize. The 3D cases are very similar, with the only difference being that the wave function is multiplied by the lowest harmonic oscillator function with frequency $2\omega_0$ in the Z direction.

First, we show the spin-singlet case using $\omega_0 = 1$. The

energy of the relative motion is $\epsilon = 1$ a.u. in this case (see the Table in Ref.⁵³). The state with $j = 0$ CM wave function is spherically symmetric for small λ (Fig. 1a), and as the anharmonicity of the harmonic oscillator dominates ($\omega_V \ll \omega_U$), a slightly ellipsoidal structure appears (Fig. 1b). For $j = 1$, the CM state is multiplied by U ($H_1(\sqrt{\omega_U}U) = 2\sqrt{\omega_U}U$) and becomes elongated in the diagonal direction (Fig. 1c). This direction is set by the choice of $\boldsymbol{\lambda} = (\lambda, \lambda)$, and other values would change the direction (see Appendix A). For larger λ , the confinement by ω_U is much stronger and the elongation disappears (Fig. 1d). For higher j values the elongation increases due to the higher $H_j(\sqrt{\omega_U}U)$ polynomials (Figs. 1e and 1g). Higher λ values decrease the elongation (Figs. 1f and 1h). This trend continues for even higher j values as well. Solutions with other ω_0 values show very similar behaviors.

In the spin-triplet case in 2D we choose $\omega_0 = 1/3$ a.u., and the energy of the relative motion is $\epsilon = 1$ a.u. Fig. 2 shows the densities for this case. This system is more sensitive to the choice of λ and we use three different λ values (0.01, 0.5, 2) to illustrate that. In this case, the spin function is symmetric, the spatial part is antisymmetric ($m = \pm 1$ in Eq. (1.2) in Ref.⁵³) and the two peaks appear in the density plot for $j = 0$ as shown in Figs. 2a, 2b and 2c. By increasing λ the U oscillator squeezes the electrons closer and the separation between the two peaks is more visible (the density between the peaks being lower). There are three peaks for $j = 1$ for $\lambda = 0.01$ and $\lambda = 0.5$, but as the U confinement gets stronger the two peak structure returns (Figs. 2d, 2e, and 2f). The three-peak structure can be a non-trivial consequence because, unlike the simple spherical structure in the singlet state, the relative motion function, in this case, is in an $m = 1$ state and multiplied by U . If we neglect the Coulomb interaction, then the relative motion wave function is a ground state harmonic oscillator for the first electron (one density peak) and the first excited harmonic oscillator state for the second electron (two peaks). These three peaks are magnified when the relative wave function is multiplied by the center of mass wave function, which is now proportional to $H_1(\sqrt{\omega_U}U) = 2\sqrt{\omega_U}U$.

For higher j states, the elongation caused by H_j continues (see Figs. 2g and 2k), and the nodal structure of H_j also contributes to the density structure. Overall it seems that the $\lambda = 0.01$ case captures the general trend very well. For larger λ values the same structures appear later as j increases. For a given j , increasing λ squeezes the elongation due to the ω_U confinement, as in the singlet case.

The total wave function will be a linear combination of the $\phi(\mathbf{r})\psi_j(\mathbf{R})|n\rangle$ components. The probability of a given component is given by

$$P_j(n) = |c_{jn}^0|^2 \quad (3.1)$$

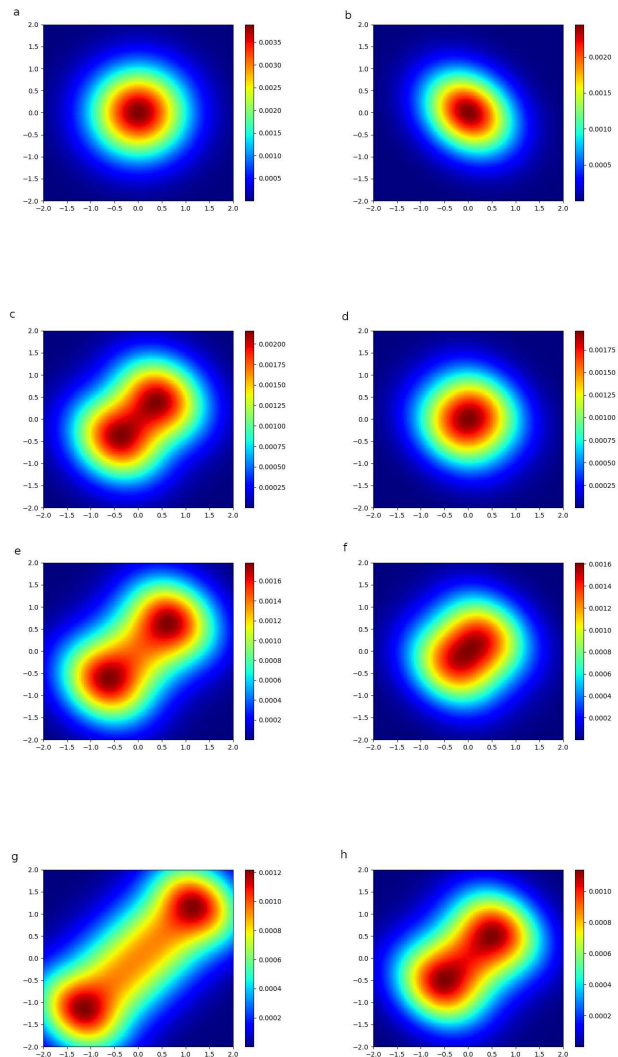


FIG. 1: Two-dimensional densities $(\phi(\mathbf{r})\psi_j(\mathbf{R}))^2$ of two electrons confined by a harmonic potential with $\omega_0 = 1$ a.u. and spin $S = 0$. First row: $j=0$, (a) $\lambda = 0.5$, (b) $\lambda = 2$. Second row: $j=1$, (c) $\lambda = 0.5$, (d) $\lambda = 2$. Third row: $j=2$, (e) $\lambda = 0.5$, (f) $\lambda = 2$. Fourth row: $j=5$, (g) $\lambda = 0.5$, (h) $\lambda = 2$.

and depends on ω_0, ω and λ . An example for $P_j(n)$ is given in Fig. 3a. First, we note that due to the structure in Eq. (2.34), the probabilities follow a checkerboard-like structure: odd photon numbers couple to odd j and even photon numbers couple to even j . The probabilities decrease for large photon numbers. The low CM excitations, $j = 0, 1, 3$, are the most dominant terms for low photon numbers. The probability of the higher CM excitations ($j = 2, 3, 4, 5$) first increases with the photon number, then reaches a maximum and starts to decrease.

Fig. 3b shows the sum $P_n = \sum_j P_n(j)$. By increasing λ , the higher photon spaces are coupled and the occupation of lower photon numbers increases. However, the

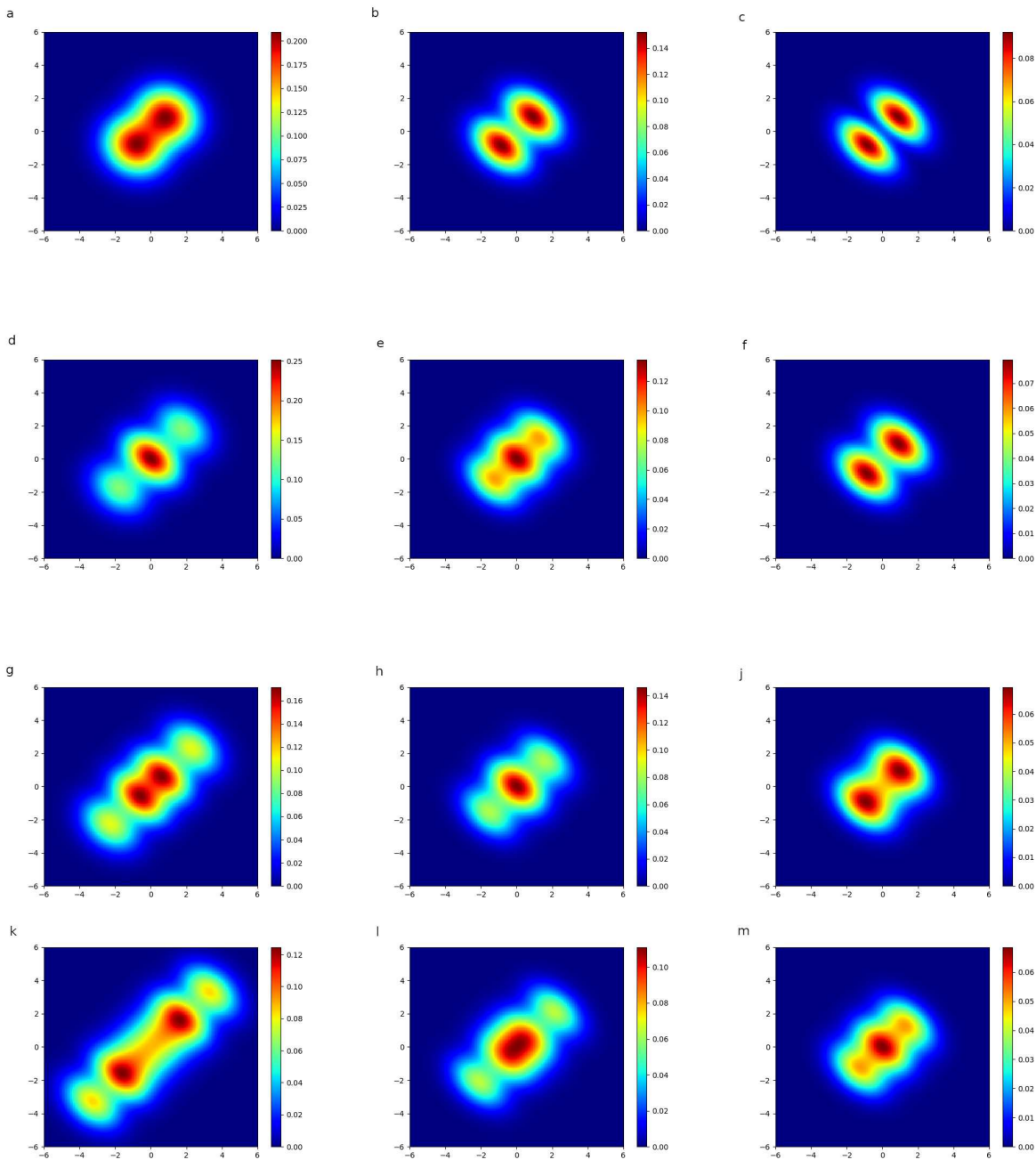


FIG. 2: Two-dimensional densities $(\phi(\mathbf{r})\psi_j(\mathbf{R}))^2$ of two electrons confined by a harmonic potential with $\omega_0 = 1/3$ a.u. and spin $S = 1$. First row: $j = 0$, (a) $\lambda = 0.01$, (b) $\lambda = 0.5$, (c) $\lambda = 2$. Second row: $j = 1$, (d) $\lambda = 0.01$, (e) $\lambda = 0.5$, (f) $\lambda = 2$. Third row: $j = 2$, (g) $\lambda = 0.01$, (h) $\lambda = 0.5$, (j) $\lambda = 2$. Fourth row: $j = 5$, (k) $\lambda = 0.01$, (l) $\lambda = 0.5$, (m) $\lambda = 2$.

effect of ω is more complicated. The coupling increases as $\sqrt{\omega}$ but with larger photon frequency the photon harmonic oscillator states move higher in energy ($n\hbar\omega$) and their occupation decreases. This latter effect seems to be dominant for smaller λ . In Fig. 3b, in case of $\lambda = 0.5$ a.u., P_n is the same for $n = 0, 1$ for $\omega = 0.5$ a.u. and $\omega = 5$ a.u., but for higher n , P_n is much smaller for

$\omega = 5$ a.u. For higher λ values this effect becomes less important. The oscillations (the even states have higher occupation than the odd states) in the case of $\omega=0.5$, $\lambda=5$ a.u. always appear when ω is much smaller than λ and probably due to the checkerboard-like coupling.

Fig. 3c shows the sum $P_j = \sum_n P_n(j)$. By increasing ω , the occupations of the low photon number states

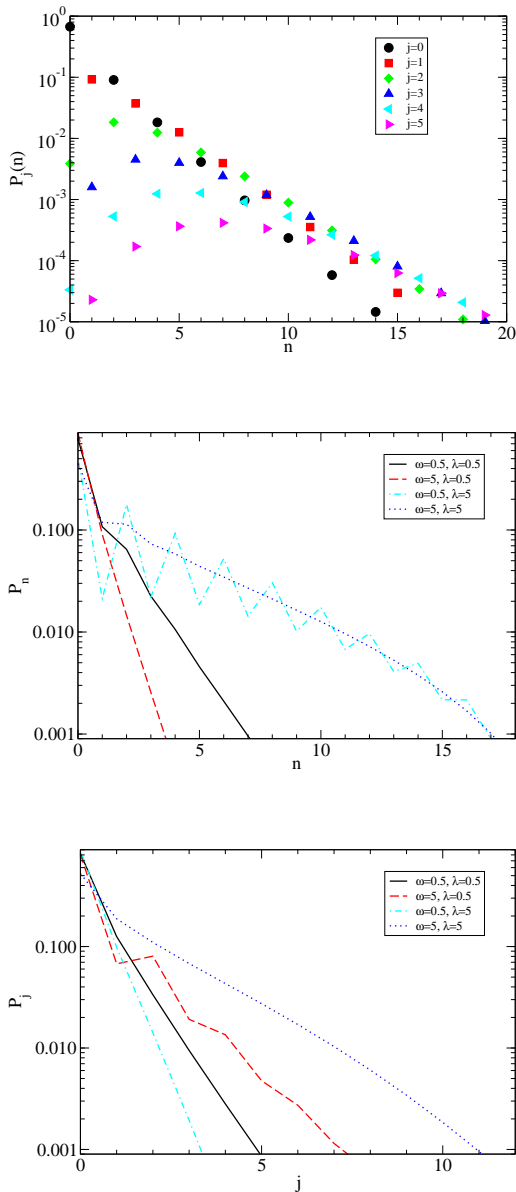


FIG. 3: Top: Probability of the occupation of a jn subspace ($\lambda = 0.5$ a.u. and $\omega = 0.5$ a.u.), $P_j(n)$. Middle: $P_n = \sum_j P_n(j)$. Bottom: $P_j = \sum_n P_n(j)$. $\omega_0 = 1/3$ a.u. is used in the calculations.

decrease and the occupations of the higher states increase. Increasing λ increases ω_U and pushes the CM states higher, and those states do not couple with the low j sector, so increasing λ decreases P_j . The effect of λ is similar to ω in the previous case: λ increases the coupling, but larger λ means larger ω_u and the CM states are pushed higher. For low ω , increasing λ relaxes the occupation, but for large ω , the coupling dominates and the λ increases the occupation of the higher n states.

Fig. 4 shows the energy of the singlet state as a function of photon frequency. The ground state energy is 3 a.u. in this case. Infinitely many photon states and in-

finitely many CM states can couple to this state. Without coupling of the photons to the center of mass, the energy of the photon states increases linearly with ω and the energy of the CM states increases linearly with ω_U . Fig. 4 shows the lowest 20 states with coupling, and we use $\lambda = \alpha\sqrt{\omega}$, which means that the coupling g is proportional to ω . For $\alpha = 1$ (Fig. 4a), some states (primarily photon states) move linearly up with ω for small frequencies, while other states (primarily CM states) only slowly increase with ω and converge to a horizontal line. To magnify the behavior we redo the calculation with $\alpha = 1/20$ (Fig. 4b). In this case, λ increases much less while we increase ω . ω_U barely changes while ω ascends from 0 to 5. The lowest state does not change (it barely couples to photons $n > 0$) and remains a horizontal line, which is just the lowest CM state. The second state increases with ω , but then it reaches the energy of the first excited CM state of energy $\hbar\omega_U \approx \hbar\omega_0$ and becomes a horizontal line. The third state also increases until it reaches the energy of the first excited state and continues on that line until meeting the second state. To avoid crossing, it moves to the second excited state of the center of mass and so on. Of course, these states do not lie exactly on horizontal lines but rise gradually with λ . For much higher ω , one can recover a similar picture to Fig. 4a.

To complete the energy spectrum of the system, one has to include the excited states of the relative motion. As those states are orthogonal, the complete spectrum can be obtained by shifting the energy levels in Fig. 4 by the energies of the excited states.

The wavefunction of the system will be a linear combination of wave functions shown in Figs. 1 and 2, with coefficients defined in the second line of Eq. (2.36). These coefficients depend on the values of ω , ω_0 , and λ . For a single photon mode, the lowest states often dominate and it is hard to pick parameters that favor a single j CM mode or higher j values. In Fig. 5a we present an example for the triplet case where the square of the linear coefficients are 0.55, 0.18, 0.10, 0.06, 0.04, 0.03 ($j=0, \dots, 5$), so a few $j \neq 0$ contribute to the density. Figs. 5b, 5c and 5d show the square of the wave function in the $n = 1, 3$ and 5 spaces. The $n=0$ density is very similar to Fig. 2b. The squares of the linear coefficients in n space are 0.49, 0.13, 0.11, 0.07, 0.05 ($n = 0, \dots, 5$). This example shows that the spatial wave functions in different photon subspaces can be very different and quantum mechanical methods have to look for accurate wave functions in different photon spaces.

The calculation can be extended to many photon modes as it is shown in Appendix A. Examples of two-photon mode calculations are shown in Figs. 6 and 7. In particular, Fig. 6 shows the photon occupation numbers for the two-photon modes, ω and 2ω . The occupation probability tilts toward the ω axis, showing that the ω modes have higher probabilities than the 2ω ones. Fig. 7 is the same calculation as is shown in Fig. 4a, but with two-photon modes. Overall, the two figures are very similar. The two-photon case reaches higher energies and

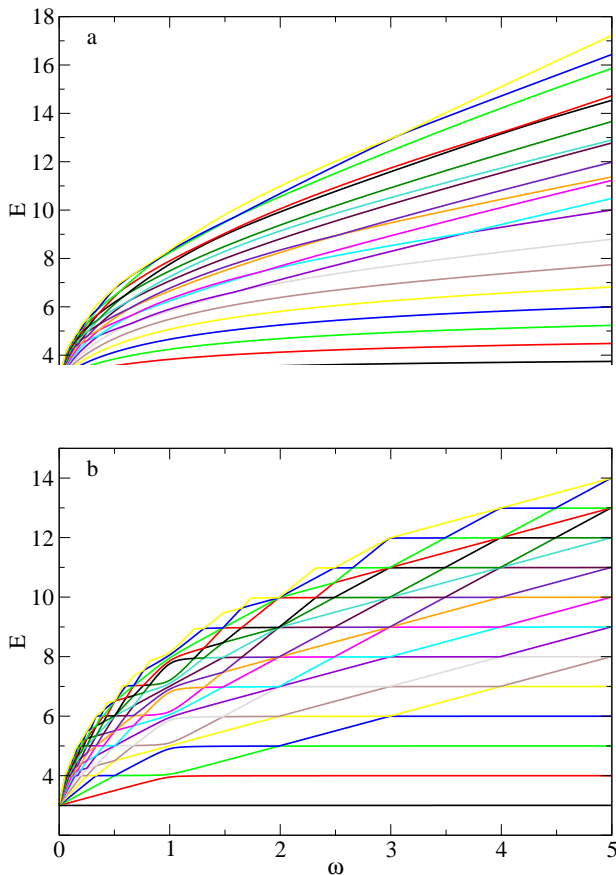


FIG. 4: Energy levels as a function of ω for (a) $\lambda = \sqrt{\omega}$ and (b) $\lambda = \sqrt{\omega}/20$, $\omega_0=1$ a.u. in both cases.

there are more level crossings. This is because some of the states shown in Fig. 7 are 2ω states and move higher faster. Increasing the number of photon modes helps to reach higher j states and multiphoton modes might be a way to select higher j states or single out a desired j value.

IV. SUMMARY

In a harmonically confined two-electron system, the light couples to the dipole moment which is proportional to the CM coordinate. By separating the relative and center of mass motion, we have shown that the coupled photon center of mass system can be solved by diagonalization and the relative motion part has analytical solutions for certain frequencies.

The coupling of the light to the center of mass coordinate leads to elongated wave functions. The symmetry axis of the electron density is determined by the polarization direction. The density has several peaks depending on the center of mass excitation and the symmetry axis of the density is determined by the polarization direction. The competition between the confinement due to the coupling to light and the node structure of the center

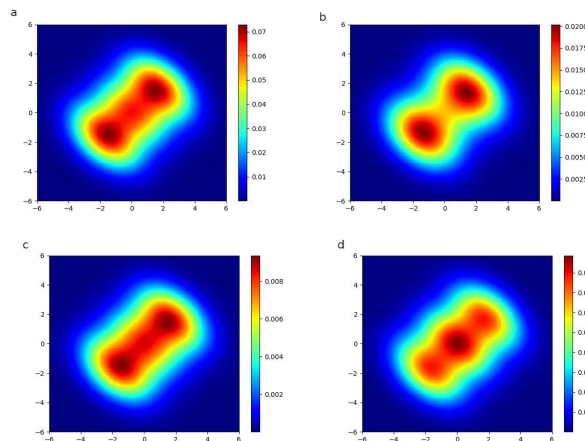


FIG. 5: Two-dimensional density $\Phi(\mathbf{r}, \mathbf{R})^2$ for the $S = 1$ case, (a) total density, (b) density in the $n = 1$ space, (c) density in the $n = 3$ space, (d) density in the $n = 5$ space. ($\omega_0 = 0.18055$ a.u., $\omega = 1$ a.u. and $\lambda = 1$ a.u.).

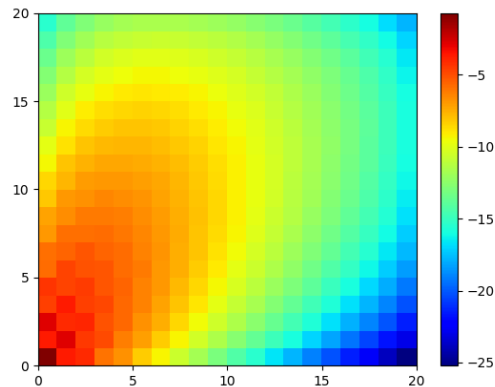


FIG. 6: Occupation numbers for the photon modes. The photon frequencies are ω and 2ω . The coupling vectors are $\boldsymbol{\lambda}$ and $-\boldsymbol{\lambda}$. The vertical axis is the photon number for ω , the horizontal axis is the photon number for 2ω ($\omega_0=1$ a.u., $\omega = 1$ a.u., $\lambda = 1$ a.u.).

of mass excitation influences the location of the density peaks.

We have shown that the spatial wave functions belonging to different photon spaces are very different, and this means that quantum mechanical approaches solving coupled light-matter problems have to determine the wave functions in each photon subspace, which might be a difficult task.

The approach can be extended to many photon modes and the only limitation is the dimension of the Hamiltonian matrix. As this matrix is very sparse, one can easily diagonalize it even for very large matrices.

As there are only very few light-matter coupled systems with analytical solutions, the present work might

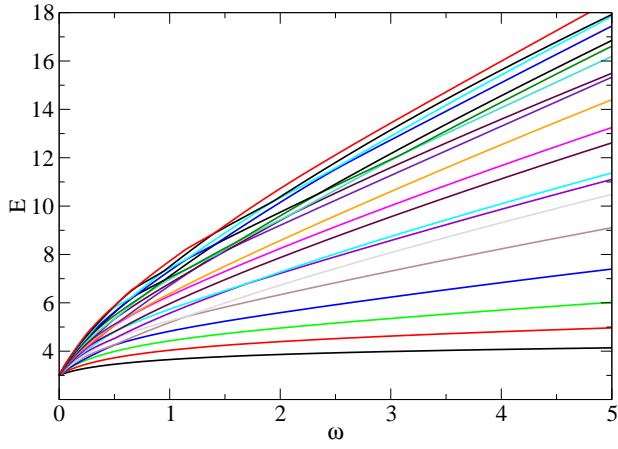


FIG. 7: Energy levels as a function of ω for the two photon modes. The photon frequencies are ω and 2ω , the coupling vectors are $\boldsymbol{\lambda}$ and $-\boldsymbol{\lambda}$, with $\lambda = \sqrt{\omega}$ ($\omega_0=1$ a.u.)

be useful to test and develop efficient approximations.

A similar approach can be used for a larger electron number, but then the relative motion part has to be solved numerically.

Appendix A: N_p photon modes

Consider the same system as in Section II A 2, except that here n_p photons are coupled. Hence, there are $N_p = 2n_p$ photon modes involved.

$$|\vec{n}\rangle = |n_1, n_2, \dots, n_{N_p}\rangle. \quad (\text{A1})$$

Define the vector Kronecker delta as

$$\delta_{\vec{n}\vec{m}} = \prod_{k=1}^{N_p} \delta_{n_k m_k}, \quad (\text{A2})$$

$$\delta_{\vec{n}\vec{m}}^l = \prod_{k=1, k \neq l}^{N_p} \delta_{n_k m_k}. \quad (\text{A3})$$

It is straightforward to generalize Eq. (2.34)

$$\langle \vec{m}, \phi_i | H | \vec{n}, \phi_j \rangle = \delta_{\vec{m}\vec{n}} \delta_{ij} (j + \frac{1}{2}) \omega_U + \delta_{\vec{m}\vec{n}} \delta_{ij} \sum_{k=1}^{N_p} (n_k + \frac{1}{2}) \omega_k + \sum_{k=1}^{N_p} \sqrt{\frac{2\omega_k}{\omega_U}} \lambda D_{n_k m_k} D_{ij} \delta_{\vec{n}\vec{m}}^k. \quad (\text{A4})$$

Appendix B: Center-of-mass motion for many photons

We assume $N_p = 2n_p$ photon modes, and λ_α 's are not necessarily isotropic in the x, y -directions. Thus, the Hamiltonian becomes

$$H = -\frac{1}{2}\nabla_1^2 + \frac{1}{2}\omega_0^2 \mathbf{r}_1^2 - \frac{1}{2}\nabla_2^2 + \frac{1}{2}\omega_0^2 \mathbf{r}_2^2 + \frac{q_1 q_2}{|\mathbf{r}_1 - \mathbf{r}_2|} + \frac{1}{2} \sum_{\alpha=0}^{N_p} (q_1 \lambda_\alpha \cdot \mathbf{r}_1 + q_2 \lambda_\alpha \cdot \mathbf{r}_2)^2. \quad (\text{B1})$$

Still imposing $q_1 = q_2$, the radial part remains unchanged and can be solved by Ref^{19,20,53}. Now we solve the CM part. Eq. (2.14) becomes

$$\left[-\frac{1}{2}\nabla_{\mathbf{R}}^2 + \frac{1}{2}\omega_{\mathbf{R}}^2 \mathbf{R}^2 + 4 \sum_{\alpha=0}^{N_p} (\lambda_\alpha \cdot \mathbf{R})^2 \right] \xi(\mathbf{R}) = \eta' \xi(\mathbf{R}). \quad (\text{B2})$$

Suppose $\lambda_\alpha = (\lambda_{\alpha 1}, \lambda_{\alpha 2}, 0)$. Further define

$$\begin{aligned} \tilde{\lambda}_1 &= \sum_{\alpha=0}^{N_p} \lambda_{\alpha 1}^2, \\ \tilde{\lambda}_2 &= \sum_{\alpha=0}^{N_p} \lambda_{\alpha 2}^2, \\ \tilde{\lambda}_{12} &= \sum_{\alpha=0}^{N_p} \lambda_{\alpha 1} \lambda_{\alpha 2}, \end{aligned} \quad (\text{B3})$$

Eq. (2.16) and (2.17) now read

$$H_{\mathbf{R}} = -\frac{1}{2} \frac{\partial^2}{\partial X^2} - \frac{1}{2} \frac{\partial^2}{\partial Y^2} + \frac{1}{2} \omega_X^2 X^2 + \frac{1}{2} \omega_Y^2 Y^2 + \frac{1}{2} \omega_{XY} XY, \quad (\text{B4})$$

where

$$\begin{aligned} \omega_X^2 &= \omega_{\mathbf{R}}^2 + 8\tilde{\lambda}_1, \\ \omega_Y^2 &= \omega_{\mathbf{R}}^2 + 8\tilde{\lambda}_2, \\ \omega_{XY} &= 16\tilde{\lambda}_{12}. \end{aligned} \quad (\text{B5})$$

This linearly coupled Hamiltonian can be easily decoupled with the following unitary transformation

$$\begin{aligned} U &= \frac{1}{(1-ab)^{1/2}} (X + aY), \\ V &= \frac{1}{(1-ab)^{1/2}} (bX + Y), \end{aligned} \quad (\text{B6})$$

where

$$\begin{aligned} a &= \frac{(\tilde{\lambda}_1 - \tilde{\lambda}_2) + \sqrt{(\tilde{\lambda}_1 - \tilde{\lambda}_2)^2 + 4\tilde{\lambda}_{12}^2}}{2\tilde{\lambda}_{12}}, \\ b &= -\frac{(\tilde{\lambda}_1 - \tilde{\lambda}_2) + \sqrt{(\tilde{\lambda}_1 - \tilde{\lambda}_2)^2 + 4\tilde{\lambda}_{12}^2}}{2\tilde{\lambda}_{12}}. \end{aligned} \quad (\text{B7})$$

In this case, the decoupled Hamiltonian reads

$$H_{\mathbf{R}}(U, V) = -\frac{1}{2} \frac{\partial^2}{\partial U^2} - \frac{1}{2} \frac{\partial^2}{\partial V^2} + \frac{1}{2} \omega_U^2 U^2 + \frac{1}{2} \omega_V^2 V^2, \quad (\text{B8})$$

where

$$\begin{aligned} \omega_U &= \sqrt{\omega_{\mathbf{R}}^2 + 4(\tilde{\lambda}_1 + \tilde{\lambda}_2) + 4\sqrt{(\tilde{\lambda}_1 - \tilde{\lambda}_2)^2 + 4\tilde{\lambda}_{12}^2}}, \\ \omega_V &= \sqrt{\omega_{\mathbf{R}}^2 + 4(\tilde{\lambda}_1 + \tilde{\lambda}_2) - 4\sqrt{(\tilde{\lambda}_1 - \tilde{\lambda}_2)^2 + 4\tilde{\lambda}_{12}^2}}. \end{aligned} \quad (\text{B9})$$

Same as in Eq. (2.19), this is just the Hamiltonian for two non-interacting harmonic oscillators. Hence, the

energies for the CM part are

$$\eta = \frac{1}{2}\eta' = \frac{1}{2}(n_U + \frac{1}{2})\omega_U + \frac{1}{2}(n_V + \frac{1}{2})\omega_V, \quad n_U, n_V = 0, 1, 2, \dots \quad (\text{B10})$$

and the ground state energy is

$$\eta_0 = \frac{1}{4}(\omega_U + \omega_V). \quad (\text{B11})$$

Finally, the corresponding wave function is just the product of that of the two independent harmonic oscillators.

Acknowledgments

This work has been supported by the National Science Foundation (NSF) under Grant No. IRES 1826917.

* Electronic address: kalman.varga@vanderbilt.edu

- 1 F. Buchholz, I. Theophilou, S. E. B. Nielsen, M. Ruggenthaler, and A. Rubio, *ACS Photonics* **6**, 2694 (2019).
- 2 C. Schäfer, M. Ruggenthaler, H. Appel, and A. Rubio, *Proceedings of the National Academy of Sciences* **116**, 4883 (2019), ISSN 0027-8424, <https://www.pnas.org/content/116/11/4883.full.pdf>, URL <https://www.pnas.org/content/116/11/4883>.
- 3 M. Ruggenthaler, N. Tancogne-Dejean, J. Flick, H. Appel, and A. Rubio, *Nature Reviews Chemistry* **2**, 0118 (2018), ISSN 2397-3358, URL <https://doi.org/10.1038/s41570-018-0118>.
- 4 J. Flick, M. Ruggenthaler, H. Appel, and A. Rubio, *Proceedings of the National Academy of Sciences* **112**, 15285 (2015), ISSN 0027-8424, <https://www.pnas.org/content/112/50/15285.full.pdf>, URL <https://www.pnas.org/content/112/50/15285>.
- 5 J. Flick, M. Ruggenthaler, H. Appel, and A. Rubio, *Proceedings of the National Academy of Sciences* **114**, 3026 (2017), ISSN 0027-8424, <https://www.pnas.org/content/114/12/3026.full.pdf>, URL <https://www.pnas.org/content/114/12/3026>.
- 6 V. Rokaj, D. M. Welakuh, M. Ruggenthaler, and A. Rubio, *Journal of Physics B: Atomic, Molecular and Optical Physics* **51**, 034005 (2018), URL <https://doi.org/10.1088/1361-6455/aa9c99>.
- 7 N. Rivera, J. Flick, and P. Narang, *Phys. Rev. Lett.* **122**, 193603 (2019), URL <https://link.aps.org/doi/10.1103/PhysRevLett.122.193603>.
- 8 J. Flick and P. Narang, *Phys. Rev. Lett.* **121**, 113002 (2018), URL <https://link.aps.org/doi/10.1103/PhysRevLett.121.113002>.
- 9 N. M. Hoffmann, L. Lacombe, A. Rubio, and N. T. Maitra, *The Journal of Chemical Physics* **153**, 104103 (2020).
- 10 I. V. Tokatly, *Phys. Rev. B* **98**, 235123 (2018), URL <https://link.aps.org/doi/10.1103/PhysRevB.98.235123>.
- 11 J. Galego, F. J. Garcia-Vidal, and J. Feist, *Phys. Rev. Lett.* **119**, 136001 (2017), URL <https://link.aps.org/doi/10.1103/PhysRevLett.119.136001>.
- 12 A. Mandal, S. Montillo Vega, and P. Huo, *The Journal of Physical Chemistry Letters* **11**, 9215 (2020), pMID: 32991814.
- 13 L. S. Cederbaum and A. I. Kuleff, *Nature Communications* **12**, 4083 (2021), ISSN 2041-1723, URL <https://doi.org/10.1038/s41467-021-24221-6>.
- 14 T. Szidarovszky, G. J. Halász, A. G. Császár, L. S. Cederbaum, and A. Vibók, *The Journal of Physical Chemistry Letters* **9**, 6215 (2018).
- 15 Y. Ashida, A. m. c. İmamoğlu, and E. Demler, *Phys. Rev. Lett.* **126**, 153603 (2021), URL <https://link.aps.org/doi/10.1103/PhysRevLett.126.153603>.
- 16 N. Rivera and I. Kaminer, *Nature Reviews Physics* **2**, 538 (2020), ISSN 2522-5820, URL <https://doi.org/10.1038/s42254-020-0224-2>.
- 17 A. Le Boité, *Advanced Quantum Technologies* **3**, 1900140 (2020), <https://onlinelibrary.wiley.com/doi/pdf/10.1002/qute.201900140>, URL <https://onlinelibrary.wiley.com/doi/abs/10.1002/qute.201900140>.
- 18 F. J. Garcia-Vidal, C. Ciuti, and T. W. Ebbesen, *Science* **373** (2021), ISSN 0036-8075, <https://science.sciencemag.org/content/373/6551/eabd0336.full.pdf>, URL <https://science.sciencemag.org/content/373/6551/eabd0336>.
- 19 M. Taut, *Phys. Rev. A* **48**, 3561 (1993), URL <https://link.aps.org/doi/10.1103/PhysRevA.48.3561>.
- 20 M. Taut, *Journal of Physics A: Mathematical and General* **27**, 1045 (1994), URL <https://iopscience.iop.org/article/10.1088/0305-4470/27/3/045>.
- 21 M. Taut, *Journal of Physics A: Mathematical and General* **28**, 2081 (1995), URL <https://iopscience.iop.org/article/10.1088/0305-4470/28/7/021>.
- 22 J. Karwowski and G. Pestka, *Theoretical Chemistry Accounts* **118** (2007), URL <https://link.springer.com/content/pdf/10.1007/s00214-007-036>.
- 23 V. M. Villalba and R. Pino, *Physics Letters A* **238**, 49 (1998), URL <https://www.sciencedirect.com/science/article/pii/S037596019800040>.
- 24 J. Karwowski, *Journal of Physics: Conference Series* **104** (2008), URL <https://iopscience.iop.org/article/10.1088/1742-6596/104/1/014001>.
- 25 A. Turbiner, *Communications in Mathematical Physics* **118**, 467 (1988), URL <https://projecteuclid.org/journals/communications-in-mathematical-physics>.
- 26 L. Liu and Q. Hao, *Theoretical and Mathematical Physics* **183** (2015), URL <https://link.springer.com/content/pdf/10.1007/s11232-015-029>.
- 27 C. A. Downing and M. E. Portnoi, *Physical Review B* **94** (2016), URL <https://journals.aps.org/prb/pdf/10.1103/PhysRevB.94.045430>.
- 28 C.-L. Ho and V. R. Khalilov, *Phys. Rev. A* **61** (2000), URL <https://journals.aps.org/pra/pdf/10.1103/PhysRevA.61.032104>.
- 29 C.-M. Chiang and C.-L. Ho, *Journal of Mathematical Physics* **43**, 43 (2002), URL <https://aip.scitation.org/doi/abs/10.1063/1.1418426>.
- 30 Y.-Z. Agboola, Davis; Zhang, *Modern physics letters A* **27** (2012), URL <https://www.worldscientific.com/doi/pdf/10.1142/2FS021773231>.
- 31 J. Karwowski and H. Witek, *Molecular Physics* **114** (2016), URL <https://www.tandfonline.com/doi/pdf/10.1080/00268976.2015.111>.
- 32 K. Akhmedov and N. Guseinova, *Russian Physics Journal* **52**, 321 (2009), URL <https://link.springer.com/content/pdf/10.1007/s11182-009-923>.
- 33 F. M. Pont, O. Osenda, and P. Serra, *Journal of Physics A: Mathematical and General* **51** (2018), URL <https://iopscience.iop.org/article/10.1088/1751-8121/aab85e/>.
- 34 C. A. Downing, *Physical Review A* **95** (2017), URL <https://journals.aps.org/pra/pdf/10.1103/PhysRevA.95.022105>.
- 35 P.-F. Loos and P. M. W. Gill, *Physical Review Letters* **108** (2012), URL <https://journals.aps.org/prl/pdf/10.1103/PhysRevLett.108.083001>.
- 36 G.-J. Guo, Z.-Z. REN, B. ZHOU, and X.-Y. GUO, *International Journal of Modern Physics B* **26** (2012), URL <https://www.worldscientific.com/doi/pdf/10.1142/2FS021797921>.
- 37 P.-F. Loos and P. M. W. Gill, *Physical Review Letters* **103** (2009), URL <https://doi.org/10.1103/PhysRevLett.103.123008>.
- 38 P.-F. Loos and P. M. W. Gill, *Molecular Physics* **108** (2010), URL <https://www.tandfonline.com/doi/pdf/10.1080/00268976.2010.508>.
- 39 R. Jestädt, M. Ruggenthaler, M. J. T. Oliveira, A. Rubio, and H. Appel, *Advances in Physics* **68**, 225 (2019).
- 40 A. Frisk Kockum, A. Miranowicz, S. De Liber-

- ato, S. Savasta, and F. Nori, *Nature Reviews Physics* **1**, 19 (2019), ISSN 2522-5820, URL <https://doi.org/10.1038/s42254-018-0006-2>.
- ⁴¹ C. Schäfer, M. Ruggenthaler, and A. Rubio, *Phys. Rev. A* **98**, 043801 (2018), URL <https://link.aps.org/doi/10.1103/PhysRevA.98.043801>.
- ⁴² J. Flick, C. Schäfer, M. Ruggenthaler, H. Appel, and A. Rubio, *ACS Photonics* **5**, 992 (2018).
- ⁴³ D. Sidler, M. Ruggenthaler, H. Appel, and A. Rubio, *The Journal of Physical Chemistry Letters* **11**, 7525 (2020), pMID: 32805122, URL <https://doi.org/10.1021/acs.jpcllett.0c01556>.
- ⁴⁴ L. Lacombe, N. M. Hoffmann, and N. T. Maitra, *Phys. Rev. Lett.* **123**, 083201 (2019), URL <https://link.aps.org/doi/10.1103/PhysRevLett.123.083201>.
- ⁴⁵ G. M. Andolina, F. M. D. Pellegrino, V. Giovannetti, A. H. MacDonald, and M. Polini, *Phys. Rev. B* **100**, 121109 (2019), URL <https://link.aps.org/doi/10.1103/PhysRevB.100.121109>.
- ⁴⁶ M. Schuler, D. D. Bernardis, A. M. Läuchli, and P. Rabl, *SciPost Phys.* **9**, 66 (2020), URL <https://scipost.org/10.21468/SciPostPhys.9.5.066>.
- ⁴⁷ A. Settineri, O. Di Stefano, D. Zueco, S. Hughes, S. Savasta, and F. Nori, *Phys. Rev. Research* **3**, 023079 (2021), URL <https://link.aps.org/doi/10.1103/PhysRevResearch.3.023079>.
- ⁴⁸ V. Rokaj, M. Ruggenthaler, F. G. Eich, and A. Rubio, *The free electron gas in cavity quantum electrodynamics* (2021), 2006.09236.
- ⁴⁹ S. Shin and H. Metiu, *The Journal of Chemical Physics* **102**, 9285 (1995), URL <https://doi.org/10.1063/1.468795>.
- ⁵⁰ A. Mandal, T. D. Krauss, and P. Huo, *The Journal of Physical Chemistry B* **124**, 6321 (2020), pMID: 32589846.
- ⁵¹ E. A. Power, S. Zienau, and H. S. W. Massey, *Philosophical Transactions of the Royal Society of London. Series A, Mathematical and Physical Sciences* **251**, 427 (1959), <https://royalsocietypublishing.org/doi/pdf/10.1098/rsta.1959.0008>, URL <https://royalsocietypublishing.org/doi/abs/10.1098/rsta.1959.0008>.
- ⁵² M. Ruggenthaler, J. Flick, C. Pellegrini, H. Appel, I. V. Tokatly, and A. Rubio, *Phys. Rev. A* **90**, 012508 (2014), URL <https://link.aps.org/doi/10.1103/PhysRevA.90.012508>.
- ⁵³ (2021), see Supplemental Material at.